Zebrafish MiR-430 Promotes Deadenylation and Clearance of Maternal mRNAs

Antonio J. Giraldez,[1,2]* Yuichiro Mishima,[3] Jason Rihel,[1,2] Russell J. Grocock,[4] Stijn Van Dongen,[4] Kunio Inoue,[3] Anton J. Enright,[4] Alexander F. Schier[1,2]*

MicroRNAs (miRNAs) comprise 1 to 3% of all vertebrate genes, but their in vivo functions and mechanisms of action remain largely unknown. Zebrafish miR-430 is expressed at the onset of zygotic transcription and regulates morphogenesis during early development. By using a microarray approach and in vivo target validation, we find that miR-430 directly regulates several hundred target messenger RNA molecules (mRNAs). Most targets are maternally expressed mRNAs that accumulate in the absence of miR-430. We also show that miR-430 accelerates the deadenylation of target mRNAs. These results suggest that miR-430 facilitates the deadenylation and clearance of maternal mRNAs during early embryogenesis.

MicroRNAs (miRNAs) are small RNA molecules that base pair with target mRNAs to induce posttranscriptional gene repression (*1*, *2*). MiRNAs have important roles during animal development. Interfering with miRNA processing by using mutants for the ribonuclease (RNase) III enzyme Dicer affects morphogenesis during zebrafish embryogenesis and mouse limb development (*3*, *4*). Modulating the function of individual miRNAs leads to defects that range from aberrant cell fate specification and cell death to abnormal cell function (*1*, *2*, *5*, *6*). Despite this progress, it is still poorly understood how miRNAs regulate developmental processes. In particular, the in vivo targets of miRNAs are largely unknown.

Several strategies have been used to identify miRNA targets (*7*). Genetic approaches have identified several miRNA-mRNA target pairs that play important roles during *Caenorhabditis elegans* development (*1*, *2*, *5*, *6*, *8*–*10*). This approach preferentially identifies targets whose reduced activity suppresses miRNA loss-of-function phenotypes. In silico target predictions based on conserved complementarity between miRNAs and orthologous mRNAs have identified ~100 to 200 putative targets for a given miRNA (*7*, *11*–*18*). It is unknown how many true but nonconserved targets are missed in this approach. Cell culture studies have used microarrays to compare mRNA levels in the presence or absence of a transfected miRNA (*19*). This method has led to the identification of ~100 putative targets for miR-1 and miR-124. It is unclear how many of the in silico or cell culture targets are regulated in vivo. Hence, developing an in vivo system to identify a large fraction of biologically relevant miRNA targets could provide major insights into the roles of miRNAs during development.

Zebrafish embryos deficient for maternal and zygotic Dicer activity (MZ*dicer*) cannot generate mature miRNAs (*3*). These mutants display defects during gastrulation and brain morphogenesis. These defects are rescued by injection of processed miRNAs belonging to the miR-430 family. MiR-430 is the most abundant miRNA family expressed during early zebrafish development (*3*, *20*), is conserved in other vertebrates (miR-302 and miR-372) (*3*), and accumulates during the maternal-to-zygotic transition. This transition is a universal process in animal development, when the embryo activates zygotic gene expression and thus no longer solely relies on maternally provided transcripts (*21*). The activation of zygotic transcription coincides with the elimination of many maternal mRNAs by unknown mechanisms. The results presented here indicate that miR-430 accelerates the deadenylation and clearance of several hundred maternal transcripts during zygotic stages.

MiR-430 accelerates target mRNA decay. Recent studies have suggested that miRNAs do not only inhibit productive translation but also affect target mRNA levels (*19*, *22*, *23*). To distinguish between effects on gene transcription and mRNA decay, we investigated the stability of a miR-430 reporter mRNA in the presence or the absence of miR-430. The reporter contained green fluorescent protein (GFP) and imperfect target sites for miR-430 in the 3′ untranslated region (UTR) (3xIPT-miR-430) (Fig. 1, A and B) and was injected shortly after fertilization. Reporter mRNA started to decay after 4 hours postfertilization (hpf) in wild-type embryos, following miR-430 accumulation after the onset of zygotic transcription (~2.5 hpf) (fig. S1). In contrast, reporter mRNA decay was delayed in the absence of miR-430 in

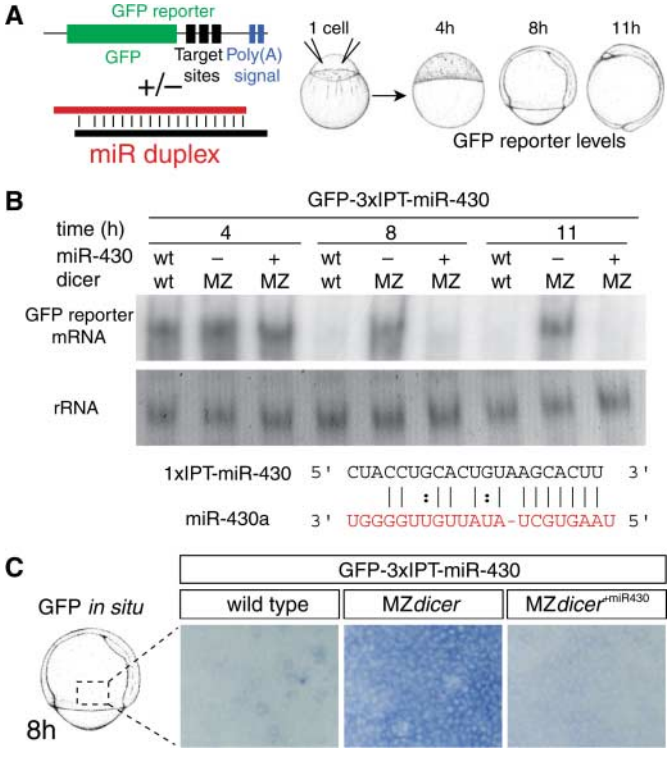

Fig. 1. MiRNAs accelerate target mRNA decay. (**A**) Experimental approach to analyze mRNA target decay in presence or absence of miRNAs. GFP reporter contains three miRNA target sites and is injected at the one-cell stage. (**B**) Northern blot of miR-430 reporter mRNA in the presence or the absence of miR-430. (**C**) In situ analysis (dark blue) of reporter mRNA in the presence or the absence of miR-430 at 8 hpf. The photos show a detail of the dorsal-lateral margin of the embryo (black rectangle, left). Note the higher reporter levels in the absence of miR-430 (fig. S2).

[1]Developmental Genetics Program, Skirball Institute of Biomolecular Medicine, and Department of Cell Biology, New York University School of Medicine, New York, NY 10016, USA. [2]Department of Molecular and Cellular Biology, Harvard University, 16 Divinity Avenue, Cambridge, MA 02138, USA. [3]Department of Biology, Graduate School of Science and Technology, Kobe University, 1-1 Rokkodaicho, Nadaku, Kobe 657-8501, Japan. [4]Wellcome Trust Sanger Institute, Hinxton, Cambridge CB10 1SA, UK.

*To whom correspondence should be addressed. E-mail: schier@fas.harvard.edu (A.F.S.); giraldez@mcb.harvard.edu (A.J.G.)

A

	≥2fold	1.5-2fold	1.2-1.5fold	Unchanged	<0.8 fold	Whole Array
Probes	275	536	330	2749	713	12754
3'UTR	118	210	133	1293	359	5219*
Target sites	88	115	50	139	17	952

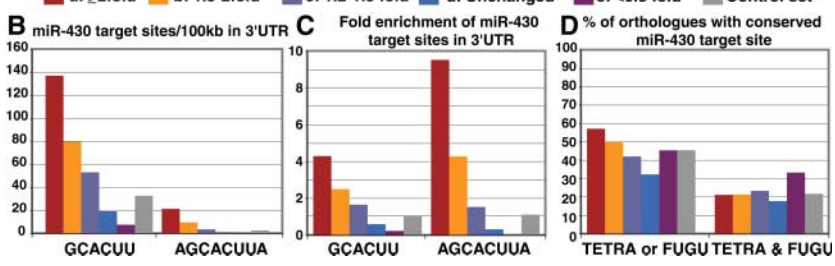

Fig. 2. MiR-430-regulated mRNAs are enriched for miR-430 target sites. (**A**) Comparison of mRNA expression levels between MZ*dicer* mutants, MZ*dicer*$^{+miR\text{-}430}$, and wild type. Columns summarize the number of probes, number of mRNAs with known 3′ UTRs, and number of mRNAs with known 3′ UTRs containing a putative miR-430 target site [defined by a hexamer (or more) sequence complementary to the miR-430 seed]. The asterisk marks the control set used for subsequent analyses. (**B** and **C**) Number (B) or -fold enrichment (C) of hexamer or octamer miR-430 target sites per 100 kb of 3′ UTR in different groups (B) and compared with the control set (C). (**D**) Percentage of mRNAs that have a hexamer (or more) miR-430 target site in the orthologous genes in *F. rubripes* (Fugu) and *T. nigroviridis* (Tetra) (fig. S3, S4, and S8).

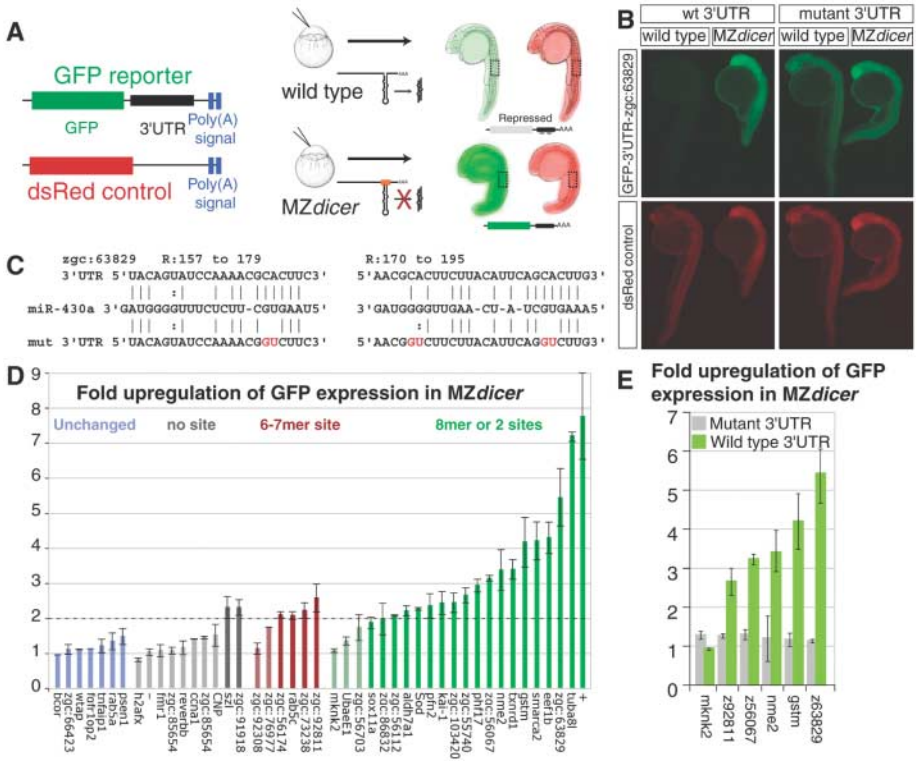

Fig. 3. miR-430 target validation. (**A**) Experimental approach. GFP reporter mRNA is co-injected with control dsRed mRNA into wild type and MZ*dicer* mutants. GFP reporter contains a 3′ UTR that is wild-type or mutant for the miR-430 target sites. (**B**) GFP reporter expression (green) and control dsRed expression (red) at 25 to 30 hpf. Wild-type reporter is repressed in wild-type embryos compared with MZ*dicer* mutants. Mutation of miR-430 target sites abolishes repression of the reporter in wild-type embryos. (**C**) Predicted pairing between wild-type or mutant target 3′ UTR and a member of the miR-430 family. (**D** and **E**) -Fold increase of GFP expression in MZ*dicer* mutants compared to wild type. Regulation was considered significant when the GFP reporter was up-regulated ≥ twofold [solid color in (D); see fig. S5, S7, and Materials and Methods for details]. Error bars indicate ± SD; $n \geq 2$; ≥15 embryos per experiment.

MZ*dicer* mutants (Fig. 1, B and C). Injection of processed miR-430 into MZ*dicer* mutants (MZ*dicer*$^{+miR\text{-}430}$) restored accelerated decay. Similar results were obtained with miR-1 and its reporter mRNA (fig. S2) (*3*). These results indicate that miRNAs can accelerate the decay of target mRNAs in vivo.

Identification of putative miR-430 targets by microarray analysis. Because miR-430 can accelerate the decay of an artificial target mRNA, we speculated that bona fide in vivo targets accumulate in the absence of miR-430. By using gene expression microarrays, we compared mRNA levels in embryos that lack miR-430 (MZ*dicer*) with those of embryos that have miR-430 (wild type and MZ*dicer*$^{+miR\text{-}430}$) (fig. S3 and table S1). More than 750 mRNAs (represented by 811 probes in the array) were present at significantly higher levels (≥1.5-fold) in MZ*dicer* mutants (Fig. 2A, fig. S3, and table S1). To determine whether these mRNAs might be direct or indirect miR-430 targets, we analyzed whether up-regulated mRNAs were enriched for putative miR-430 target sites. Such sites are complementary to the 5′ seed region of miR-430, which is crucial for target recognition (*14*, *15*, *24*–*26*). We performed this analysis for the 328 up-regulated mRNAs that had experimentally identified 3′ UTRs (Fig. 2A, fig. S3, and Materials and Methods) and a control data set containing the 5219 genes on the array with defined 3′ UTRs. On the basis of the rules developed by Lewis *et al*. (*14*), we searched for sequences complementary to a hexamer seed (positions 2 to 7 in the seed), a septamer seed, or an octamer seed (with an adenosine at the 3′ end of the target sequence) (*14*). mRNAs with increased levels in MZ*dicer* mutants had significantly more predicted target sites per 100 kb in their 3′ UTRs compared with those of the control set (Fig. 2B). This translated into a ~4- to ~10-fold enrichment compared with the control set (Fig. 2C) and a ~10- to ~30-fold enrichment when compared with the set of mRNAs that remained unchanged in the array (Fig. 2C). No enrichment was found for sequences complementary to the miRNA seeds of let-7 or miR-1 (fig. S4). These results suggest that the group of mRNAs whose levels were increased more than 1.5-fold in MZ*dicer* mutants is greatly enriched for miR-430 targets.

MiR-430 target validation. To validate putative targets, we tested miR-430-dependent regulation of reporters consisting of GFP and full-length 3′ UTRs (Fig. 3A). First, we analyzed whether GFP expression from the reporter was higher in MZ*dicer* mutants compared with that of wild type. Second, we assessed whether repression of the GFP reporter in wild-type embryos depended on the miR-430 target sites in the 3′ UTR. We co-injected GFP reporter mRNAs and control mRNAs encoding the red fluorescent protein (dsRed) and compared the GFP levels in wild type and MZ*dicer* mutants

at 25 to 30 hpf (Fig. 3, fig. S5, and Materials and Methods). We considered an mRNA to be regulated by miR-430 when the normalized GFP reporter expression in MZ*dicer* was increased more than twofold compared with wild type. Between 92% and 71% of the tested putative targets were up-regulated in vivo in the absence of miR-430 (n = 37) (Fig. 3, B to D, and figs. S5 and S6). For example, we validated 12 of 13 (92%) mRNAs with two or more target sequences complementary to miR-430 seeds, six of eight (75%) mRNAs with one octamer target site, and five of seven (71%) mRNAs with one hexamer or septamer target site. In contrast, none of the tested mRNAs that were unchanged in the array and lacked miR-430 sites were repressed in wild type compared to MZ*dicer* (n = 7).

To test for direct regulation by miR-430, we mutated two nucleotides in the predicted target site in the 3′ UTR of five putative targets (GCACUU to GGUCUU) (Fig. 3, B, C, and E, and fig. S7). This strongly reduced or abolished repression in wild-type embryos in all cases (Fig. 3E and fig. S7), suggesting that most if not all the 3′ UTRs validated in MZ*dicer* mutants are likely to be direct miR-430 targets in vivo.

Combining the microarray data, target predictions, and validation results led to the identification of a group of 101 mRNAs that have a greater than 85% probability to be direct miR-430 targets (figs. S3 and S7). Members of this group were up-regulated ≥1.5-fold in MZ*dicer* mutants and had one octamer target site or two target sites (hexa-, septa-, or octamer) in their 3′ UTRs. Even the 102 mRNAs that were up-regulated ≥1.5-fold and had one hexamer or septamer target site had a 71% probability to be miR-430 targets (figs. S3 and fig. S6). Hence, we estimate that miR-430 directly regulates ~160 mRNAs of a target set of 203 mRNAs with defined 3′ UTRs (table S1 and fig. S6). Because 3′ UTRs were only available for roughly half (328 of ~750) of the up-regulated mRNAs, we extrapolate that miR-430 might directly regulate more than 300 of these mRNAs (fig. S6). If we also take into account that the array covers less than half of all predicted zebrafish genes, we estimate that miR-430 directly regulates several hundred target mRNAs during early zebrafish development.

MiR-430 targets are not preferentially conserved. Computational identification of miRNA targets often relies on the principle that conserved miRNAs have conserved targets (*1*, *7*). We therefore asked how many of the 203 genes in the zebrafish miR-430 target set have a hexamer miR-430 target site in the 3′ UTR of orthologous genes in two other teleosts, *Fugu rubripes* and *Tetraodon nigroviridis* (fig. S8 and table S1). As described in Materials and Methods, we estimate that ~50% of our experimentally identified target sites are found in the orthologous genes in either *Fugu* or *Tetraodon* and only ~25% are conserved in all three species (Fig. 2D and fig. S8). Regulation mediated by the 3′ UTR of conserved and nonconserved targets resulted in similar posttranscriptional regulation of the GFP reporter (fig. S8). These results suggest a very rapid evolution of the miR-430 target set and indicate that a large fraction of bona fide targets for miR-430 and other miRNAs (*18*) would be missed if conservation were used as the sole criterion.

Most miR-430 target mRNAs are expressed maternally. To investigate whether the 203 mRNAs in the miR-430 target set share specific features, we analyzed their expression profile and gene ontology (GO). No significant differences in the distribution of GO classes were found for genes in the target set compared to the entire genome (fig. S9). We then compared the expression profile of genes in the miR-430 target set with genes in the control set that were expressed during early embryogenesis. About 40% of the target set mRNAs but only ~10% of the control set mRNAs were present at high levels at 1.5 hpf but at low levels at 5 and 9 hpf (Fig. 4A and fig. S10). These are mRNAs deposited into the egg by the mother before fertilization, because the genome is transcriptionally silent until ~2.5 hpf (*21*, *27*). In the absence of miR-430, the maternal transcripts in the target set accumulated to higher levels than in wild-type embryos (table S1). In addition to the fourfold enrichment of predominantly maternal transcripts in the miR-430 target set, ~40% of predominantly maternal mRNAs (162 out of 402) were predicted to have miR-430 target sites compared with only 18% in the control set (Fig. 4C and fig. S10). Hence, not only was the miR-430 target set enriched for maternal mRNAs, but maternal mRNAs were also enriched for miR-430 target sites. Another ~50% of the target mRNAs were expressed both maternally and zygotically. In particular, half of these targets maintained steady levels zygotically (Fig. 4B and fig. S10) but accumulated to higher levels in the absence of miR-430 (table S1). Taken together, the analysis of miR-430 targets indicates that miR-430 accelerates the clearance of several hundred maternal and maternal-zygotic mRNAs.

MiR-430 promotes target mRNA deadenylation. The polyadenosine [poly(A)] tail stabilizes mRNAs and enhances cap-dependent translation (*28*–*31*). Upon fertilization, many maternally deposited mRNAs become polyadenylated and competent for translation, whereas deadenylation triggers translational silencing and decay (*28*–*30*). We therefore tested whether miRNA-induced target decay correlates with changes in the length of the poly(A) tail of reporter and endogenous target mRNAs. Time course analysis of injected target mRNAs revealed that polyadenylation is followed by rapid deadenylation that is induced by miR-430 and results in complete deadenylation at about 6 hpf (~3 hours after the onset of miR-430 accumulation) (Fig. 5 and fig. S11). Three controls indicated that rapid deadenylation is miRNA-mediated. First, mutation of miR-430 target sites in the 3′ UTR delayed target deadenylation (Fig. 5, A to D). Second, deadenylation of target mRNAs is delayed in MZ*dicer* mutants, similar to non-miRNA targets or GFP alone (Fig. 5, D to F,

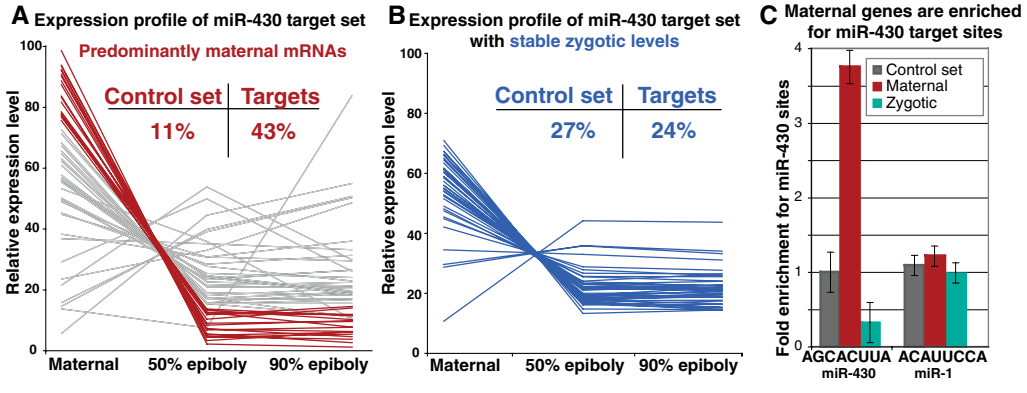

Fig. 4. MiR-430 facilitates the clearance of maternal transcripts. (**A** and **B**) Relative expression profile of mRNAs at 1.5 (maternally provided mRNAs), 5, and 9 hpf. (**A**) Expression profile of 50 mRNAs in the miR-430 target set. Predominantly maternal mRNAs are highlighted in red. The miR-430 target set is fourfold enriched for predominantly maternal mRNAs when compared with a random set of mRNAs (fig. S10). (**B**) Expression profile of 50 mRNAs in the miR-430 target set that are present at different levels maternally but show stable levels during zygotic stages (blue). The mRNAs in the miR-430 target set accumulate to higher levels in the absence of miR-430 (table S1). (**C**) -Fold enrichment of octamer target sites for miR-430 and miR-1 in the control set, predominantly maternal mRNAs, and predominantly zygotic mRNAs. About 40% of the predominantly maternal mRNAs have a hexamer miR-430 target site (see Materials and Methods for details regarding maternal and zygotic mRNAs).

and fig. S11). Third, injection of miR-430 into MZ*dicer* mutants accelerates target deadenylation (Fig. 5, D and F). Similar results were observed for different endogenous and reporter miR-430 targets (fig. S11) as well as reporters partially complementary to miR-1 (Fig. 5G).

To test whether miRNA-induced target deadenylation is a secondary effect of nonproductive translation, we repressed GFP reporter expression by using morpholino antisense oligonucleotides that hybridize to the translational start site. This did not cause reporter mRNA decay or deadenylation to the same extent as the miRNA did (Fig. 5G). Furthermore, miRNA-induced deadenylation still occurred in the absence of translation (Fig. 5G). Taken together, these results indicate that miR-430 accelerates target deadenylation and mRNA decay.

The study of miR-430 in vivo targets provides three major insights. First, miR-430 directly regulates several hundred target mRNAs during early embryogenesis. These targets are up-regulated in MZ*dicer* mutants, contain miR-430 target sites, and can be validated in vivo. Although the number of identified miR-430 targets is high, it is likely that there are additional targets that were not identified in our approach. These targets might include mRNAs that are expressed at low levels, regulated by miR-430 during other developmental stages, or regulated at the level of translation rather than transcript stability. Our results provide in vivo support for in silico and cell culture studies that have predicted large sets of putative miRNA targets (*7*, *11*–*19*, *31*). However, 50% of the miR-430 target set would have been missed by relying on conservation, a criterion that is often used in computational approaches. Moreover, it remains unclear how many of the in silico or cell culture targets are biologically relevant targets in vivo. In contrast, in vivo approaches using miRNA loss-of-function combined with target validation identify bona fide targets.

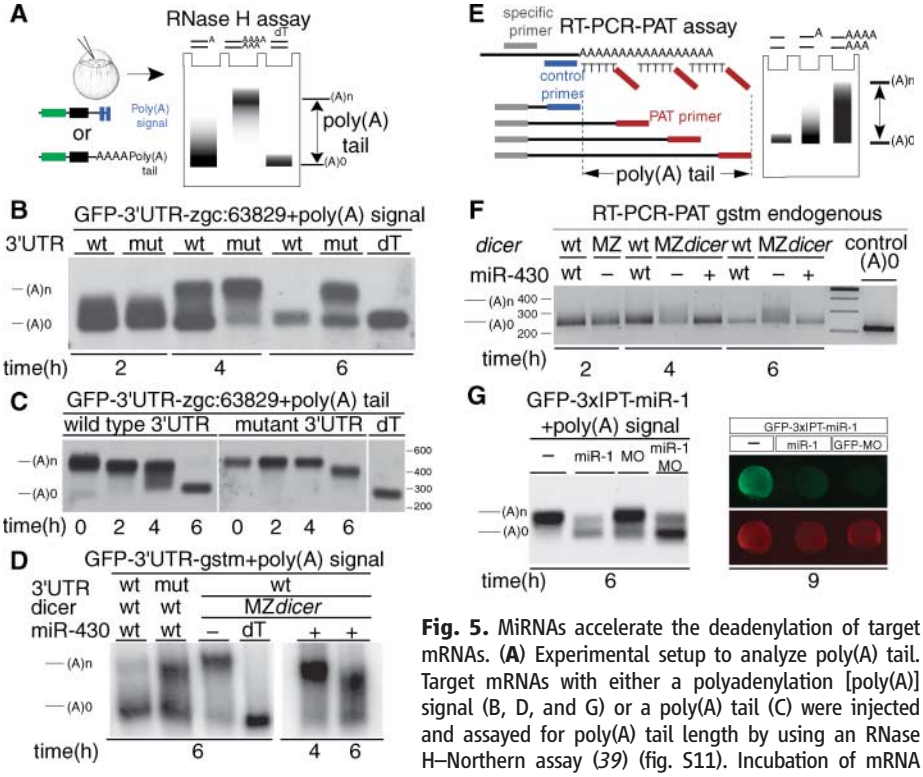

Fig. 5. MiRNAs accelerate the deadenylation of target mRNAs. (**A**) Experimental setup to analyze poly(A) tail. Target mRNAs with either a polyadenylation [poly(A)] signal (B, D, and G) or a poly(A) tail (C) were injected and assayed for poly(A) tail length by using an RNase H–Northern assay (*39*) (fig. S11). Incubation of mRNA with oligodeoxythymidine (dT) and RNase H tests the mobility of the deadenylated RNA fragment. (**B** to **D**) Northern analysis of poly(A) tail length of GFP reporter mRNA with wild-type (wt) or mutant (mut) target sites in the 3′ UTR in the presence or absence of miR-430. GFP reporter mRNA is polyadenylated between 0 and 4 hpf (B). Deadenylation of wild-type GFP reporter is accelerated compared with that of GFP reporters with mutated miR-430 target sites (B and C) and in wild type compared with MZ*dicer* mutants (D). Accelerated deadenylation can be partially rescued in MZ*dicer* mutants by injecting miR-430 duplexes (D) (fig. S11). (**E**) Method used to detect poly(A) tail length of endogenously expressed target mRNAs, reverse transcription polymerase chain reaction (RT-PCR) poly(A) test (PAT). The length of the smear reveals the approximate size of the poly(A) tail. (**F**) Time course RT-PCR PAT of endogenous miR-430 targets in the presence of endogenous (wt), injected miR-430 (+), or absence of miR-430 (MZ*dicer*, –). Note the shortening of the poly(A) tail in the presence of miR-430 (see Materials and Methods for details). (**G**) RNaseH-Northern assay of a GFP reporter for miR-1 in the presence or absence of translational repression by antisense morpholino (MO). MiR-1 and MO repress GFP translation (green), but miR-1 preferentially accelerates deadenylation.

Second, our results suggest a critical role for miR-430 in the maternal-to-zygotic transition during embryogenesis. In all animals, the mother deposits mRNAs into the egg. Upon fertilization, maternal mRNAs are activated and translated, whereas the genome is transcriptionally silent until a later stage (*21*, *28*–*30*). Because maternally provided transcripts cannot be repressed at the transcriptional level, posttranscriptional and posttranslational mechanisms are required to regulate their activity (*28*–*30*). MiR-430 is expressed at the onset of zygotic transcription and accelerates the deadenylation and decay of a large set of maternal mRNAs (fig. S12). The accumulation of these maternal transcripts is the likely cause of the developmental delay and gastrulation defects observed in MZ*dicer* mutants (*3*). MiRNA-induced clearance of maternal mRNAs might be a universal mechanism to regulate the maternal-to-zygotic transition. Our analysis of miR-430 and its targets might also have wider implications for miRNA function during development. MiR-430 is involved in a developmental transition (maternal-to-zygotic), but, even without miR-430 and despite the delayed clearing of maternal mRNAs, the embryo can still activate its zygotic program (e.g., embryonic patterning). Hence, lack of miR-430 does not arrest the embryo in a maternal state but results in a mixed maternal-zygotic state. This suggests that miR-430 and other miRNAs might not exclusively function as switches from one state (B) to the next state (C) but might sharpen developmental transitions and counteract the formation of mixed states (B-C) (fig. S12). This model has important implications for the role of miRNAs in disease. Premature expression of miRNAs might aberrantly target mRNAs required to specify state B, thus maintaining cells in an earlier state A (fig. S12). Such a mechanism might account for the miRNA-mediated induction of cancer (*2*). Our findings also provide a framework to interpret recent studies that have indicated that specific miRNAs and their predicted target mRNAs tend to be expressed in a mutually exclusive manner (*17*, *18*). These and previous results (*19*, *32*) have led to the hypotheses that miRNAs confer robustness by targeting erroneously transcribed genes or by preventing premature or prolonged mRNA accumulation. Our results provide in vivo support for the latter hypothesis, suggesting that miRNAs target mRNAs that might otherwise persist during later stages. In addition, a fraction of the target mRNAs continues to be coexpressed with miR-430 after the maternal-to-zygotic transition. These target mRNAs are not eliminated but modulated by miR-430. Thus, miR-430 accelerates the clearance of maternal mRNAs and dampens the levels of maternal-zygotic mRNAs.

Third, our study suggests that miR-430 accelerates deadenylation of target mRNAs and thus provides a potential mechanism for miRNA function. The poly(A) tail confers mRNA stabil-

ity and stimulates translation via the interaction of poly(A) binding protein (PABP) with the 5′ m7G cap (*28*–*30*). Previous studies have found that miRNAs inhibit Cap-dependent translation (*33*) and induce mRNA degradation (*19*, *22*, *23*, *34*). We therefore postulate that miRNA-induced deadenylation is one of the mechanisms by which miRNAs enhance target decay and repress productive translation (fig. S12). Although it remains to be determined whether deadenylation is the primary step in mRNA regulation, we observed that block of translation does not accelerate mRNA deadenylation to the same extent as the miRNA does. It is therefore conceivable that miRNAs induce the deadenylation of their targets, which results in the block of translation and the recruitment to processing bodies (P-bodies), where mRNAs are decapped and degraded (*33*–*38*). Taken together, our results suggest that miRNAs promote the deadenylation and decay of hundreds of target mRNAs and thus sharpen and accelerate the transition between developmental states.

References and Notes

1. D. P. Bartel, *Cell* **116**, 281 (2004).
2. I. Alvarez-Garcia, E. A. Miska, *Development* **132**, 4653 (2005).
3. A. J. Giraldez *et al.*, *Science* **308**, 833 (2005); published online 17 March 2005 (10.1126/science.1109020).
4. B. D. Harfe, M. T. McManus, J. H. Mansfield, E. Hornstein, C. J. Tabin, *Proc. Natl. Acad. Sci. U.S.A.* **102**, 10898 (2005).
5. R. C. Lee, R. L. Feinbaum, V. Ambros, *Cell* **75**, 843 (1993).
6. B. J. Reinhart *et al.*, *Nature* **403**, 901 (2000).
7. E. C. Lai, *Genome Biol.* **5**, 115 (2004).
8. B. Wightman, I. Ha, G. Ruvkun, *Cell* **75**, 855 (1993).
9. H. Grosshans, T. Johnson, K. L. Reinert, M. Gerstein, F. J. Slack, *Dev. Cell* **8**, 321 (2005).
10. R. J. Johnston, O. Hobert, *Nature* **426**, 845 (2003).
11. A. Stark, J. Brennecke, R. B. Russell, S. M. Cohen, *PLoS Biol.* **1**, E60 (2003).
12. A. J. Enright *et al.*, *Genome Biol.* **5**, R1 (2003).
13. B. John *et al.*, *PLoS Biol.* **2**, e363 (2004).
14. B. P. Lewis, C. B. Burge, D. P. Bartel, *Cell* **120**, 15 (2005).
15. B. P. Lewis, I. H. Shih, M. W. Jones-Rhoades, D. P. Bartel, C. B. Burge, *Cell* **115**, 787 (2003).
16. A. Krek *et al.*, *Nat. Genet.* **37**, 495 (2005).
17. A. Stark, J. Brennecke, N. Bushati, R. B. Russell, S. M. Cohen, *Cell* **123**, 1133 (2005).
18. K. K.-H. Farh *et al.*, *Science* **310**, 1817 (2005); published online 22 November 2005 (10.1126/science.1121158).
19. L. P. Lim *et al.*, *Nature* **433**, 769 (2005).
20. P. Y. Chen *et al.*, *Genes Dev.* **19**, 1288 (2005).
21. J. Newport, M. Kirschner, *Cell* **30**, 687 (1982).
22. S. Bagga *et al.*, *Cell* **122**, 553 (2005).
23. Q. Jing *et al.*, *Cell* **120**, 623 (2005).
24. E. C. Lai, *Nat. Genet.* **30**, 363 (2002).
25. J. G. Doench, P. A. Sharp, *Genes Dev.* **18**, 504 (2004).
26. J. Brennecke, A. Stark, R. B. Russell, S. M. Cohen, *PLoS Biol.* **3**, e85 (2005).
27. S. Mathavan *et al.*, *PLoS Genet.* **1**, 260 (2005).
28. J. D. Richter, *Microbiol. Mol. Biol. Rev.* **63**, 446 (1999).
29. S. Vasudevan, E. Seli, J. A. Steitz, *Genes Dev.* **20**, 138 (2006).
30. C. H. de Moor, H. Meijer, S. Lissenden, *Semin. Cell Dev. Biol.* **16**, 49 (2005).
31. J. Krutzfeldt *et al.*, *Nature* **438**, 685 (2005).
32. M. W. Rhoades *et al.*, *Cell* **110**, 513 (2002).
33. R. S. Pillai *et al.*, *Science* **309**, 1573 (2005); published online 4 August 2005 (10.1126/science.1115079).
34. R. S. Pillai, *RNA* **11**, 1753 (2005).
35. J. Liu, M. A. Valencia-Sanchez, G. J. Hannon, R. Parker, *Nat. Cell Biol.* **7**, 719 (2005).
36. L. Ding, A. Spencer, K. Morita, M. Han, *Mol. Cell* **19**, 437 (2005).
37. J. Liu *et al.*, *Nat. Cell Biol.* **7**, 1161 (2005).
38. J. Rehwinkel, I. Behm-Ansmant, D. Gatfield, E. Izaurralde, *RNA* **11**, 1640 (2005).
39. F. J. Salles, W. G. Richards, S. Strickland, *Methods* **17**, 38 (1999).

40. We thank C. Antonio, I. Baptista, V. Greco, H. Knaut, H. Lopez-Schier, S. Mango, T. Schell, and W. Talbot for providing helpful comments on the manuscript. A.J.G. was supported by European Molecular Biology Organisation and is currently supported by a Human Frontier Science Program fellowship. A.F.S. was an Irma T. Hirschl Trust Career Scientist and an Established Investigator of the American Heart Association. This work was also supported by grants from the NIH (A.F.S.). Array data has been deposited in Gene Expression Omnibus (GEO) database under accession number GSE4201.

Supporting Online Material

www.sciencemag.org/cgi/content/full/1122689/DC1
Materials and Methods
Figs. S1 to S12
Table S1(≥1.5fold).xls
Targets-tested.doc

16 November 2005; accepted 8 February 2006
Published online 16 February 2006;
10.1126/science.1122689
Include this information when citing this paper.

Evolution of the Eastern Tropical Pacific Through Plio-Pleistocene Glaciation

Kira T. Lawrence,* Zhonghui Liu, Timothy D. Herbert

A tropical Pacific climate state resembling that of a permanent El Niño is hypothesized to have ended as a result of a reorganization of the ocean heat budget ~3 million years ago, a time when large ice sheets appeared in the high latitudes of the Northern Hemisphere. We report a high-resolution alkenone reconstruction of conditions in the heart of the eastern equatorial Pacific (EEP) cold tongue that reflects the combined influences of changes in the equatorial thermocline, the properties of the thermocline's source waters, atmospheric greenhouse gas content, and orbital variations on sea surface temperature (SST) and biological productivity over the past 5 million years. Our data indicate that the intensification of Northern Hemisphere glaciation ~3 million years ago did not interrupt an almost monotonic cooling of the EEP during the Plio-Pleistocene. SST and productivity in the eastern tropical Pacific varied in phase with global ice volume changes at a dominant 41,000-year (obliquity) frequency throughout this time. Changes in the Southern Hemisphere most likely modulated most of the changes observed.

A notable inflection point in the global benthic oxygen isotope ($\delta^{18}O$) record at ~3 million years ago (Ma) marks the beginning of the Plio-Pleistocene transition (*1*). During the preceding early Pliocene interval (3 to 5.3 Ma), there was little or no ice in the Northern Hemisphere (*2*), and global mean surface temperatures were ~3°C warmer than they are today (*3*). However, at ~3 Ma, benthic $\delta^{18}O$ values and ice-rafted debris in the North Atlantic and North Pacific signal two substantial changes in high-latitude climate (*4*–*6*). The Northern Hemisphere began a period of long-term growth in continental ice, most rapidly between about 3 and 2 Ma. At the same time, the variability of high-latitude climate increased markedly, as seen by the growing amplitude of 41,000-year (41-ky) obliquity cycles in benthic $\delta^{18}O$ beginning ~3 Ma (*7*). What was the manifestation of this climatic transition in the tropics? One emerging theory is that the tropical ocean shifted from a state much like permanent El Niño before ~3 Ma to its modern, more La Niña–like state after ~3 Ma (*8*–*11*).

In the modern ocean, the ventilated thermocline (the strong vertical thermal gradient between warm surface waters and cool deep waters) in the EEP brings cold, nutrient-rich waters to the surface, which are initially derived from the sinking of mid- to high-latitude surface waters in the Southern and Northern hemispheres (*9*, *12*–*14*). This outcropping of cold, nutrient-rich water gives rise to high productivity in the EEP and sets up east-west SST and atmospheric pressure gradients, which reinforce and are reinforced by the Trade Winds. At present, mean annual SSTs are 23°C in the EEP and 29°C in the western equatorial Pacific (WEP), yielding a modern surface temperature difference of 6°C (*15*). The resulting temperature gradient and associated pressure gradients drive the strong east-west atmospheric circulation pattern (Walker Circulation). A disruption of Walker Circulation gives rise to El Niño conditions, in which weaker easterly Trade Winds and a deeper thermocline in the EEP result in a warming of surface waters and a concomitant decline in biological productivity.

A recent theory (*9*) connects the posited transition from a permanent El Niño to a La Niña climate state to a fundamental change in linkages between the high- and low-latitude ocean on long-term time scales (>10^6 years) and orbital time scales (10^4 to 10^5 years). According to this

Department of Geological Sciences, Brown University, Box 1846, Providence, RI 02912, USA.

*To whom correspondence should be addressed. E-mail: kira_lawrence@brown.edu

Zebrafish MiR-430 Promotes Deadenylation and Clearance of Maternal mRNAs

Antonio J. Giraldez *et al.*

Science **312**, 75 (2006);
DOI: 10.1126/science.1122689